LAWRENCE
LIVERMORE
NATIONAL
LABORATORY

UCRL-JRNL-201444

A versatile sol-gel synthesis route to metal-silicon mixed oxide nanocomposites that contain metal oxides as the major phase

B. J. Clapsaddle, D. W. Sprehn, A. E. Gash, J. H. Satcher, R. L. Simpson

December 14, 2003

Journal of Non-Crystalline Solids

A versatile sol-gel synthesis route to metal-silicon mixed oxide nanocomposites that contain metal oxides as the major phase

Brady J. Clapsaddle*, David W. Sprehn, Alexander E. Gash, Joe H. Satcher Jr., and Randall L. Simpson

Lawrence Livermore National Laboratory, Chemistry and Materials Science Directorate and Energetic Materials Center, Livermore, CA 94550, U.S.A.

UCRL-JRNL-201444

*Corresponding author. Address, telephone number, and e-mail: Lawrence Livermore National Laboratory, P. O. Box 808 L-092, Livermore, CA 94551; phone - +1-925-424-4254; fax: +1-925-423-4897; email - clapsaddle1@llnl.gov.

Abstract

The general synthesis of metal-silicon mixed oxide nanocomposite materials, including a variety of both main group and transition metals, in which the metal oxide is the major component is described. In a typical synthesis, the metal oxide precursor, $MCl_x \cdot yH_2O$ (x=3-6, y=0-7), was mixed with the silica precursor, tetramethylortho-silicate (TMOS), in ethanol and gelled using an organic epoxide. The successful preparation of homogeneous, monolithic materials depended on the oxidation state of the metal as well as the epoxide chosen for gelation. The composition of the resulting materials was varied from M/Si=1-5 (mol/mol) by adjusting the amount of TMOS added to the initial metal oxide precursor solution. Supercritical processing of the gels in CO_2 resulted in monolithic, porous aerogel nanocomposite materials with surface areas ranging from 100 - 800 m^2/g. The bulk materials are composed of metal oxide/silica particles that vary in size from 5 – 20 nm depending on the epoxide used for gelation. Metal oxide and silica dispersion throughout the bulk material is extremely uniform on the nanoscale. The versatility and control of the synthesis method will be discussed as well as the properties of the resulting metal-silicon mixed oxide nanocomposite materials.

PACS: 81.20.Fw; 82.70G; 82.33.Ln

1. Introduction

Metal oxide materials prepared by sol-gel chemistry are high surface area and high porosity materials that are attractive in applications such as insulators, ceramic precursors, and catalyst supports. The versatility of sol-gel chemistry provides a means

of controlling the shape, morphology and textual properties of the final material [1]. Sol-gel chemistry also provides a means of preparing mixed metal oxides in which mixing of two or more metal oxide phases can be controlled on both a molecular and a nanometer scale. Several such systems are comprised of metal oxide-silicon oxide composites that are desirable for a variety of transition and main group metals.

To date, sol-gel methods have been used to synthesize a large number of metal-silicon (M-Si) mixed oxide composites. These systems commonly contain the desired metal oxide entrapped in the silicon oxide matrix, therefore such materials contain silicon oxide as the major phase. Such materials have also required a variety of synthesis techniques depending on the metal oxide phase desired in the silica matrix. To date, there has been no generalized method for the synthesis of these M-Si composites that is reproducible and applicable to a large variety of transition and main group metal oxides.

Due to the use of metal oxides in energetic thermite reactions, M-Si mixed oxide systems have become of particular interest to us. The success of using sol-gel prepared nanocomposites as energetic materials has made it desirable to synthesize M-Si mixed oxide nanocomposites in which the transition metal oxide is the major component [2]. Recently, a general sol-gel synthetic method has been demonstrated for the synthesis of a large number of metal oxide materials towards this end [3-9]. Through the use of an organic epoxide to mediate the pH of the sol, several metal oxides have been prepared by the sol-gel method using common metal salts (Cl^-, NO_3^-, etc.) [3, 5]. Using this approach, Fe-Si mixed oxide composites in which iron(III) oxide is the major phase were recently synthesized and characterized [9].

Expanding on previous research, this report demonstrates the versatility of this method for preparing a variety of M-Si mixed oxide nanocomposites with the metal oxide as the major phase. Metal oxide/silica composites have been prepared using the silica precursor TMOS and hydrated chloride salts ($MCl_x \cdot yH_2O$; x=2-6, y=0-7) of Ni^{2+}, Al^{3+}, Sc^{3+}, V^{3+}, Cr^{3+}, Ga^{3+}, Y^{3+}, In^{3+}, Ti^{4+}, Zr^{4+}, Sn^{4+}, Hf^{4+}, Nb^{5+}, Ta^{5+}, and W^{6+} and

appears to be applicable to a large number of other metal salts, including lanthanide metal salts [9]. Following supercritical processing in CO_2, the novel M-Si mixed oxide gels formed mesoporous aerogel materials with high surface areas. Ratios of M/Si (mol/mol) were varied from 1–5 and several epoxide gelation promoters were examined. The nanocomposite materials were characterized by elemental analysis, nitrogen adsorption/desorption, Fourier transform infrared spectroscopy (FTIR), and transmission electron microscopy (TEM). In addition, energy filtered TEM (EFTEM) was used to examine the degree of mixing between the two constituents on the nanoscale. The resulting aerogel materials show evidence of a high degree of dispersion between the metal and silicon oxide components.

2. Experimental Section

All metal salts and organic epoxides were purchased from Aldrich Chemical Company. The TMOS used as the silicon oxide precursor was purchased from Gelest, Inc. All chemicals purchased were reagent grade or better and used as received. All reactions were performed in ethanol (200 proof, Aaper) under ambient conditions unless otherwise noted.

2.1. Preparation of M-Si Mixed Oxide Gels.

Reaction conditions varied slightly depending upon the metal oxide phase being synthesized. A general reaction procedure follows. In a typical reaction, the metal chloride salt (3 mmol) was dissolved while stirring in 2.5 g of 200 proof ethanol in a polyethylene vial. Depending on the hydration of the metal salt, additional water was added to the ethanolic salt solution to achieve a M/H_2O molar ratio ≥ 6. Simultaneously, the desired amount of TMOS (M/Si atomic molar ratio of 1-5) was added to a separate

2.5 g aliquot of ethanol and stirred in a separate vial. Following dissolution of the metal salt, the two solutions were combined and allowed to stir for several minutes. Once the metal chloride was dissolved, an epoxide (28 mmol) was stirred into the solution. If the epoxide used was propylene oxide (PO), it was typically added in 2 or more aliquots due to the increased reactivity observed for PO, especially with metal salts with oxidation states ≥ 4. (**CAUTION:** addition of PO to several metal salt solutions is accompanied by significant heat generation, which in some cases leads to flash boiling of the synthesis solution. The authors recommend the careful, gradual addition of PO to the solutions in a well-ventilated lab space allowing time for the solutions to cool between aliquot additions.) If instead, the epoxide was trimethylene oxide (TMO) or dimethyl oxetane (DMO), the epoxide was typically added in a single aliquot. After the addition of the epoxide, the solution was briefly stirred to ensure thorough mixing and the stir bar was then quickly removed. The reaction mixture was then covered and allowed to gel.

2.2. Processing of Fe-Si Mixed Oxide Gels.

All gels remained covered and were aged for at least 24 hours after the initial gelation. Following aging, each gel was subjected to a pore-washing/solvent exchange step in 200 proof ethanol for 3 – 5 days. During this time, the wash solution was replaced at least three times with fresh ethanol. For aerogel preparation, the solvent-exchanged gels were processed in a Polaron™ supercritical point dryer. The ethanol in the wet gel pores was exchanged for $CO_2(l)$ for 3 – 4 days at ~12 ºC. Following complete solvent exchange, the temperature of the vessel was ramped to ~45 ºC while maintaining a pressure of ~100 bar to obtain supercritical CO_2. The vessel was then depressurized at a rate of about 7 bar/hr.

2.3. Physical Characterization of Fe-Si Mixed Oxide Composites.

Elemental analyses were performed at Galbraith Laboratories, Inc. (Knoxville, TN) using standard methods for determination of C, H, N, Si, and M content.

Prior to taking FTIR spectra, samples were prepared by grinding together 1 mg of the M-Si mixed oxide aerogel with 100 mg of dry potassium bromide (Buck Scientific) with a mortar and pestle followed by pressing the mixture into a pellet. All FTIR was performed under a nitrogen purge on a ThermoNicolet Nexus 4000 spectrometer in transmission mode at 4 cm^{-1} resolution for 128 scans.

Surface area determination, pore volume, and pore size analysis were performed by BET (Brunauer-Emmett-Teller) and BJH (Barrett-Joyner-Halenda) methods using an ASAP 2000 surface area analyzer (Micromeritics Instrument Corp.) [10]. Samples of approximately 0.1-0.2 g were heated to 200 ˚C under vacuum (10–5 torr) for at least 24 h to remove all adsorbed species. Nitrogen adsorption data were taken at five relative pressures from 0.05 to 0.20 at 77K, to calculate the surface area by BET theory.

High-resolution transmission electron microscopy (HRTEM) of M-Si mixed oxide aerogels was performed on a Philips CM300FEG operating at 300 keV using zero loss energy filtering with a Gatan energy imaging filter (GIF) to remove inelastic scattering. The images were taken under bright field conditions and slightly defocused to increase contrast. The images were also recorded on a 2K × 2K CCD camera attached to the GIF.

Energy Filtered TEM (EFTEM) element maps were obtained by electron energy loss spectroscopy (EELS) in tandem with the Philips CM300FEG TEM microscope. All EELS measurements were made with a Gatan model 607 electron energy-loss spectrometer attached to the microscope. Measurements were made at the Si-$L_{2,3}$ edges as well as a suitable metal edge depending on the composite. Images were processed using Digital Micrograph™ 3.3.1 software from Gatan, Inc.

3. Results

We have previously reported the sol-gel synthesis of Fe-Si mixed oxide composites prepared by adding organic epoxides to a solution containing $FeCl_3 \cdot 6H_2O$ and tetramethylorthosilicate (TMOS) [9]. The epoxide acts as a gelation promoter by scavenging protons from solution through a ring-opening reaction with the nucleophilic anion of the Fe^{3+} salt, the mechanism of which has been discussed in detail elsewhere [5, 11]. Briefly, as protons are gradually scavenged from the system, the $[Fe(H_2O)_6]^{3+}$ ions begin to condense into a 3-dimensional network via the processes of olation and oxolation [12]. The epoxide chosen has a significant impact on the rate of proton scavenging and thus affects the subsequent processes of oxolation and olation during the condensation of the metal oxide phase.

We have recently expanded this epoxide addition method to the synthesis of M-Si mixed oxide composites using a variety of common main group and transition metal salts. The addition of an organic epoxide to an ethanolic solution of $MCl_x \cdot yH_2O$ (x=2-6, y=0-7) and TMOS resulted in gels in several cases. Figure 1 shows a summary of all the metals successfully used to date in the preparation of metal oxides and M-Si mixed oxide composites by the epoxide addition method described here and elsewhere [2, 4-6, 8, 9]. More specifically, the nanocomposites studied in this work consist of aerogels comprised of Ni^{2+}, Al^{3+}, Sc^{3+}, V^{3+}, Cr^{3+}, Ga^{3+}, Y^{3+}, In^{3+}, Ti^{4+}, Zr^{4+}, Sn^{4+}, Hf^{4+}, Nb^{5+}, Ta^{5+}, and W^{6+} oxides mixed with silica in M/Si molar ratios of 5, 2, and 1. [1] The M-Si mixed oxide composites presented here, in many cases, represent the first reported examples of M-Si mixed oxide composites in which the metal oxide is the major phase. The large number of main group and transition metal-silica composites synthesized by this method demonstrates the versatility of this synthetic procedure to a variety of binary systems.

[1] As can be seen in Figure 1, lanthanide oxides and Ln-Si composites can also be synthesized by this method, the results of which will be presented elsewhere.

Though many examples of sol-gel prepared materials using some of these compounds exist, to our knowledge, this is the first time a single synthesis method has proven as versatile for the synthesis of such a large number of compositions.

The composites were made by mixing an ethanolic metal salt solution with an ethanolic TMOS solution to form a homogeneous solution. These solutions were then gelled by adding one of the organic 1,2- or 1,3-epoxides shown in Figure 2, propylene oxide (PO), trimethylene oxide (TMO), or dimethyloxetane (DMO). After supercritical processing, porous M-Si mixed oxide aerogels were obtained and remained monolithic in most cases. Photographs of select M-Si mixed oxide aerogel monoliths can be seen in Figure 3. Elemental analysis results for the various M-Si mixed oxide materials are presented in Table 1. There is little deviation between the desired M/Si ratio and that determined experimentally. Small amounts of carbon and hydrogen (not listed) were also present in the final materials due to the organic gelation agent and solvent used in the preparation of the gels. Carbon and hydrogen, however, comprised less than 3-6 wt% of the final material in most cases.

The composite materials in this study are comprised of a metal oxide or oxyhydroxide and a silica (SiO_2) component. The specific phases of metal oxides present are not known, but are most likely a mixture of oxides and/or oxyhydroxides, depending on the oxidation state of the metal [12]. This is further supported by the presence of water and hydroxyl groups, both of which are present in the final materials as confirmed by FTIR analysis. FTIR spectra of some representative composite aerogels of M/Si=2 are shown in Figure 4. The spectra between 800 and 4000 cm^{-1} consist largely of two features, a broad signal due to the presence of OH bands (3000-3800 cm^{-1}) and the antisymmetric Si–O–Si stretch. As can be seen for the spectra of Cr-, Zr-, Nb-, and W-Si mixed oxide composites, ν_{as}(Si–O–Si) is routinely between 1040 and 1050 cm^{-1}. This frequency range is consistent for all of the M-Si mixed oxide composites presented

in this work and has previously been reported for Fe-Si mixed oxide composites as well [9].

Synthetically, it is often useful to determine the gelation time (t_{gel}) of the initial sol. In this study, t_{gel} is defined as the time between the addition of the last aliquot of epoxide and the time at which the solution ceases to discernibly flow under the influence of gravity. A summary of gelation times for representative M-Si mixed oxide composites prepared using the standard conditions described above is shown in Table 2. The gelation times are highly dependant on the epoxide used as well as the oxidation state of the metal. As has been previously demonstrated for 1,2- and 1,3-epoxides and also observed in this work, t_{gel} generally increases in the order of PO < TMO < DMO [8, 9]. For example, as shown in Table 1, M^{3+} composites generally gel within a few minutes when PO is used as the gelation promoter. The same composites synthesized using TMO take hours or days to gel. Similar results are seen for composites made with metal salts containing oxidation states > 3. In several cases, however, PO caused precipitation or localized gelation of the sol upon addition, so TMO or DMO was used to produce a homogeneous gel. For example, composites made with Hf^{4+} could be gelled using PO, but generally gelled very quickly. Gelation could be slowed by a reasonable amount by using TMO, t_{gel} = 15 minutes compared to < 1 minute for PO, making gelation easier to control. Similarities were seen in the synthesis of Nb^{5+} and Ta^{5+} composite gels; the use of PO resulted in precipitates and localized gelation, whereas TMO increased t_{gel} and homogeneous gels could be obtained. Analogously, when the synthesis of W^{6+} gels was attempted with PO or TMO, precipitates formed instead of gels. When DMO was used instead, t_{gel} = 10 minutes and a homogeneous, W-Si mixed oxide gel was formed.

Table 3 summarizes the surface areas, pore volumes, and pore diameters for the various composite aerogels. A variety of porous materials were obtained upon supercritical processing of the gels to aerogels with surface areas ranging between 90-800 m^2/g. Previously reported Fe-Si mixed oxide composites displayed surface areas ranging

from 350-450 m^2/g [9]. In general, surface area was observed to increase slightly as the M/Si ratio decreased, as is shown for Cr-Si mixed oxide aerogels in Table 3. All M-Si mixed oxide materials presented here had narrow pore size distributions and pore diameters between 2 and 20 nm. The shape of a type IV adsorption/desorption isotherm, indicative of mesoporous materials (pore diameters = 2-50 nm), was observed for all materials tested. Adsorption/desorption properties appear to vary slightly with the choice of gelation promoter. Generally, composites made with TMO displayed pore volumes and pore diameters smaller than those observed for materials of the same composition made with PO, as can be seen for Al-Si nanocomposites. This difference is less noticeable however as the oxidation state of the metal increases. For example, the surface area, pore volume, and pore diameter of Zr-Si nanocomposites (oxidation state = 4) are observed to vary little when TMO is used as the gelation agent instead of PO. Further comparison of the effect of gelation agent was difficult due to the lack of homogeneous gels obtained with PO for metals with oxidation states > 4.

The nanostructures of several aerogels listed in Figure 1 were examined using TEM and HRTEM. Figure 5 contains images for select M-Si nanocomposites aerogels. The nanocomposites display the classic aerogel structure that is comprised of nanoparticles clustered together to form a mesoporous structure. The size of the particles appears to be fairly uniform throughout the gels, with most composites having particle sizes ranging from 5 – 20 nm. A slight difference, however, was noticed between samples prepared with PO and those prepared with either TMO or DMO. Composites prepared with PO generally had a slightly smaller range of particle sizes. Particle sizes of the Cr-Si mixed oxide composite shown in Figure 4 and prepared with PO were between 5 – 9 nm, consistent with the particle sizes of other composites prepared in the same manner. The other composites pictured, W-, Nb-, and Zr-Si mixed composites gelled with TMO or DMO, had a larger, but less uniform particle size, with sizes ranging from 7 to 20 nm.

Imaging was also used to study the degree of dispersion between the two phases. Element maps of the composite materials were produced using electron energy loss spectroscopy (EELS) in tandem with TEM. The resulting energy filtered TEM (EFTEM) Si element maps of the various composites are shown in Figure 5. In the micrographs, the bright areas represent regions of the bulk material that are particularly "rich" in Si. It can be seen that the Si is uniformly dispersed throughout all the materials and no large domains of SiO_2 appears to be present. Furthermore, there appears to be a significant amount of both M and Si in a majority of the nanoparticles when compared to the individual particles that make up a specific cluster of material. Similar results were obtained when looking at other M-Si mixed oxide composites as well, although much less silicon signal was observed as the M/Si ratio was increased to five.

In addition to the composites discussed here and summarized in Figure 1, the synthesis of several other M-Si mixed oxide composites was also attempted. To date, no other composites have been successfully synthesized by the epoxide addition method. In some cases, the oxidation state of the metal dictated the materials obtained. For example, V-Si mixed oxide nanocomposites could be obtained using V^{3+} salts, but V^{5+} salts resulted in the formation of bright orange precipitates when reacted with all the epoxides investigated in this study. Formation of Mo-Si mixed oxides was also not achievable by the epoxide addition method, despite encouraging results using the other group 6 metals chromium and tungsten. In addition, it has previously been noted that with the exception of Ni^{2+}, dicationic metals do not undergo gelation by the epoxide addition method [6, 13]. The same results were also observed in this work, with the formation of bright green Ni-Si mixed oxides being the only M^{2+}-Si mixed oxide composites successfully prepared. The formation of Ni^{2+} oxide gels by the epoxide addition method is discussed elsewhere [13].

4. Discussion

We have previously reported the use of epoxides as gelation agents for the preparation of Fe-Si mixed oxide composites [9]. The epoxides in these sol-gel systems act as an irreversible proton scavenger, resulting in a uniform pH gradient, caused by the ring opening of the epoxide upon reaction with the acidic metal oxide precursor, $[M(H_2O)_y]^{x+}A_x^-$, and anion of the metal salt (shown below) [5, 8].

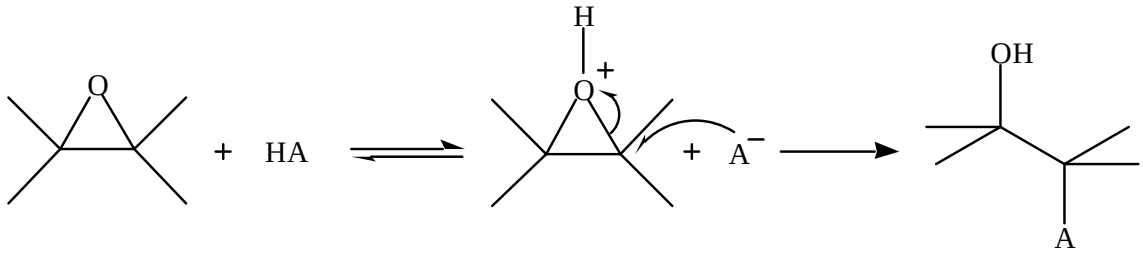

This hydrolysis of the $[M(H_2O)_y]^{x+}$ ion results in the formation of metal aquo/hydroxy, for metals with oxidation states of 3 and 4, or metal oxo/hydroxy species, for metals with oxidation states of 4-6. The formation of such species in the sol results in the initiation of the condensation reactions of olation and oxolation to form the metal oxide network [12].

Hydrolysis of the metal oxide precursor is required before condensation reactions can form the metal oxide network [12]. The rate of hydrolysis in the present systems is dependant on both the acidity of the aquo ligand and the ring opening reaction of the epoxide gelation agent [8]. Upon coordination of a water molecule to the metal center, the higher the oxidation state of the metal, the more acidic the water molecule will be, thus hydrolysis is expected to occur faster for metal oxide precursors with high oxidation states [14]. In addition, a 1,2-epoxide, such as propylene oxide, is much more likely to abstract a proton, due to the inherent reactivity caused by the strained 3-membered ring, as compared to a 1,3-epoxide, such as TMO or DMO, that consists of a less strained, 4-membered ring [11]. Since these two factors control the pH of the sol, the rate of the pH change can be controlled by the choice of epoxide and the oxidation state of the metal

oxide precursor. Controlling these parameters ultimately influences the homogeneity of the nanocomposites obtained by the gelation reactions.

The synthesis of the composite materials in this study demonstrates the control afforded by the epoxide addition method on the variety of compositions attainable. For example, consideration of the composites listed in Table 2 show that metals with an oxidation state of three were typically gelled using PO and had short to moderate gelation times. Composites made with Al^{3+} and Cr^{3+} and gelled with PO had t_{gel} < 10 minutes for all M/Si ratios. When Al-Si composites were gelled using TMO, t_{gel} increased to 12 hours, demonstrating the lower reactivity of the 1,3-epoxides. Shorter gelation times have also been noted for mixed oxide composites containing Fe^{3+} made with PO as compared to TMO or DMO [8, 9]. Composites made with metals having an oxidation state of four, Zr^{4+} and Hf^{4+}, could be gelled with PO, but t_{gel} < 1 minute for all M/Si ratios and resulted in weak, inhomogeneous gels. When the tetravalent metal composites were instead gelled using TMO, t_{gel} increased to 2-15 minutes and resulted in strong, homogeneous gels. Due to the higher oxidation state of four for Zr and Hf, the metal oxide precursors are more acidic, resulting in a fast hydrolysis when reacted with PO, and thus uniform gels could not be obtained. Through slowing the reaction by the use of the 1,3-epoxide TMO, however, a homogeneous gel was obtained. Similarly, Nb^{5+} and Ta^{5+} gels formed precipitates when PO was used as the gelation agent, indicating the fast, uncontrolled reaction of PO with the high oxidation state metal oxide precursors. Uniform Nb-Si or Ta-Si mixed oxide gels, however, were formed when TMO was used. Finally, all composites containing W^{6+}, the highest oxidation state metal present in this study, resulted in precipitates when using either PO or TMO, but could be gelled using the less reactive DMO. The rate of epoxide ring opening of DMO is slower than TMO due to the two methyl groups in the 2 position of the epoxide ring, thus the less reactive DMO is successful for gelling W^{6+} composites [11]. By choosing the correct epoxide,

the rates of hydrolysis of the metal oxide precursors can be modified to obtain homogeneous composite gels containing metal oxide phases with several oxidation states.

It should be noted that in general, as M/Si ratios decreased, t_{gel} generally increased, but the trends noted above for metal oxidation state and epoxide reactivity were maintained. We believe the SiO_2 precursor, TMOS, to be simultaneously hydrolyzed and condensed with the metal oxide precursors via the traditional acid catalyzed mechanism for alkoxysilanes [1, 15]. This is consistent with the acidity noted above for the nanocomposite sols. Furthermore, the low energy of ν_{as}(Si–O–Si) observed for all composites in the FTIR spectra is consistent with silica framework structures formed by an acid catalyzed mechanism. Acid hydrolyzed silica (ν_{as}(Si–O–Si) < 1070 cm^{-1}) tends to be less crosslinked than based hydrolyzed silica (ν_{as}(Si–O–Si) > 1070 cm^{-1}) [1, 15, 16]. The ν_{as}(Si–O–Si) bands observed for the composites in the current study are consistently between 1030 and 1050 cm^{-1}, much lower than energies observed for highly crosslinked silica.

Upon processing of the wet gels, the versatility of the epoxide addition method has successfully produced aerogel nanocomposite materials in which silicon oxide is contained in a large variety of metal oxide matrices. The degree of dispersion between the phases throughout the bulk material is of interest in any composite material. These materials display a good dispersion of silica throughout the metal oxide matrix without a significant degree of segregation between the two components on the nanoscale. The simultaneous condensation of the silica and metal oxide phase in a homogeneous sol is believed to be responsible for the extremely uniform distribution of the two oxide components in the nanocomposites. Both the TEM and EFTEM images shown in Figure 5 for the composites show no signs of large silica domains in the metal oxide matrix on the scales shown. In fact comparison of individual particles between the TEM bright field image and EFTEM images shows there to be a mix of both Si and M atoms in a significant number of particles. It should be noted that element maps of a large number

of M-Si mixed oxide composites could not be obtained due to overlap of EELS edge energies between silicon and the metal, therefore rendering it impossible to distinguish between Si and metal signals using EELS. All obtainable element maps, however, showed a similar degree of dispersion to the maps shown in Figure 5.

Several interesting trends were noted for the surface properties of the various materials. In general, particles size ranges were larger for gels prepared with 1,3-epoxides. A larger particle size range for composites made with 1,3-epoxides was previously observed in the preparation of Fe-Si mixed oxide composites [9]. It is believed that the longer t_{gel} observed for composites gelled with the 1,3-epoxides compared to t_{gel} for the same materials gelled with 1,2-epoxides is responsible for larger particle growth. The difference in particle size also seems to be apparent when analyzing the N_2 adsorption/desorption data presented in Table 3. For example, Al/Si=3 nanocomposites gelled with TMO displayed a surface area, pore volume, and pore diameter smaller than those observed for the same composite material gelled with PO, a variation which can be explained by larger particle sizes. The difference in surface properties and porosity between compositional composites made with different epoxides, however, appears to less pronounced for metals with higher oxidation states. For example, the Zr/Si=1 nanocomposite surface properties are essentially the same for materials prepared with PO and TMO. The similarity in these properties for Zr-Si composites gelled with PO (t_{gel} = 1 min) compared to those gelled with TMO (t_{gel} = 2 min) is consistent with the t_{gel} observed for both sets of composites made with the different epoxides. The short t_{gel} was approximately the same for both PO and TMO gelled Zr-Si composites, thus nanoparticles for each material had approximately the same amount of time for nucleation and growth in the initial sol. Further investigation of this phenomenon was limited due to inhomogeneous gelation or formation of precipitates with PO during gelation of composites comprised of higher oxidation state metals.

In general, M-Si composites with oxidation states > 3 showed moderate to small surface areas, pore volumes, and pore diameters. This is consistent with the higher amount of shrinkage observed for the materials upon supercritical processing. Metals with oxidation states of 4 and 5 were observed to shrink 50 to 80% by volume as compared to the alcogel, whereas most 3+ metal oxide composites only displayed 20 – 30% shrinkage. W-Si mixed oxide composites displayed very low surface areas, typically < 100 m^2/g, with small porosity and moderate pore diameters, 0.39 mL/g and 16.3 nm respectively.

5. Conclusions

The versatility of the epoxide addition method for the synthesis of M-Si mixed oxide nanocomposites has been described. The successful demonstration of the method showed that by changing the epoxide gelation agent, gelation conditions could be controlled to such an extent that a large number of composites that vary both in M/Si ratio and metal composition could be obtained. Such versatility resulted in successful variation of M/Si so that nanocomposites in which the metal oxide was the major component were obtained. Furthermore, due to the compositional generality of the method, the nanocomposites contained a variety of metal oxides with several oxidation states.

The final materials exhibited a uniform dispersion of the metal oxide and silica phases. The high degree of dispersion between metal oxides and silica on the nanoscale in composites that contain a metal oxide as the major phase has useful applications for energetic nanocomposite materials and is currently being explored in our laboratories. Furthermore, due to the large availability of organically functionalized silanes, the current method represents a unique way of introducing organic functionality to bulk metal oxide materials [17-18].

Acknowledgements

This work was performed under the auspices of the US Department of Energy by the University of California, Lawrence Livermore National Laboratory under contract No. W-7405-Eng-48. Special thanks go to Jennifer S. Harper for TEM analyses.

References

[1] C. J. Brinker, G. W. Scherer, Sol-Gel Science: The Physics and Chemistry of Sol-Gel Processing, Academic Press, San Diego, 1989.

[2] T. M. Tillotson, A. E. Gash, R. L. Simpson, L. W. Hrubesh, J. H. Satcher Jr., J. F. Poco, J. Non-Cryst. Solids 285 (2001) 338-345.

[3] H. Itoh, T. Tabata, M. Kokitsu, N. Okazaki, Y. Imizu, A. Tada, J. Ceram. Soc. Jpn. 101 (1993) 1081.

[4] T. M. Tillotson, W. E. Sunderland, I. M. Thomas, L. W. Hrubesh, J. Sol-Gel Sci. Technol. 1 (1994) 241-249.

[5] A. E. Gash, T. M. Tillotson, J. H. Satcher Jr., J. F. Poco, L. W. Hrubesh, R. L. Simpson, Chem. Mater. 13 (2001) 999-1007.

[6] A. E. Gash, T. M. Tillotson, J. H. Satcher Jr., L. W. Hrubesh, R. L. Simpson, J Non-Cryst. Solids 285 (2001) 22-28.

[7] W. Dong, C. Zhu, J. Mater. Chem. 12 (2002) 1676-1683.

[8] A. E. Gash, J. H. Satcher Jr., R. L. Simpson, Chem. Mater. 15 (2003) 3268-3275.

[9] B.J. Clapsaddle, A.E. Gash, J.H. Satcher Jr., R.L. Simpson, J. Non-Cryst. Solids 331 (2003) 190-201.

[10] S. J. Gregg, K. S. W. Sing, Adsorption, Surface Area, and Porosity, Academic Press, London, 1982.

[11] B. Dobinson, W. Hoffmann, B. P. Stark, The Determination of Epoxides, Pergamon Press, Oxford, 1969.

[12] J. Livage, M. Henry, C. Sanchez, Prog. Solid State Chem. 18 (1988) 259.

[13] A.E. Gash, J.H. Satcher Jr., R.L. Simpson, submitted to J. Non-Cryst. Solids, 2003.

[14] C.F. Baes, R.E. Mesmer Jr., The Hydrolysis of Cations, Wiley, New York, 1976.

[15] J.D. Wright, N.A.J.M. Sommerdijk, Sol-Gel Materials: Chemistry and Applications, Gordon and Breach Science, Amsterdam, 2001.

[16] M. Schraml-Marth, K.L. Walther, A. Wokaun, B.E. Handy, A. Baiker, J. Non-Cryst. Solids 143 (1992) 93-111.

[17] L. Zhao, B.J. Clapsaddle, J.H. Satcher Jr., K.J. Shea, manuscript in preparation.

[18] B.J. Clapsaddle, L. Zhao, A.E. Gash, J.H. Satcher Jr., K.J. Shea, M.L. Pantoya, and R.L. Simpson, MRS Proceedings, MRS Fall Meeting, Boston, MA, U.S.A., November 30 – December 5, 2003.

Figure Captions

Figure 1. Summary of the metal oxides and M-Si mixed oxide composites prepared to date by the epoxide addition method (shaded).

Figure 2. Structures of a 1,2-epoxide (PO) and 1,3-epoxides (TMO and DMO).

Figure 3. Pictures of various M-Si mixed oxide aerogel monoliths: left to right, top row, Al/Si=3, Sn/Si=2, Cr/Si=2; bottom row, Zr/Si=2, Nb/Si=5, W/Si=2. The scale in all pictures is in centimeters.

Figure 4. FTIR spectra of various M/Si=2 composites. The labels indicate the metal oxide present in each spectrum. The ν_{as}(Si–O–Si) peak for the compounds can be seen *c.a.* 1050 cm^{-1}. Peaks at energies >1000 cm^{-1} for the Nb and W composites are due to the metal oxide phase as confirmed by FTIR analysis of samples containing no SiO_2 component.

Figure 5. Bright field TEM images (left) and EFTEM Si maps (right) of a. W/Si = 2, b. Nb/Si=1, c. Zr/Si=1, and d. Cr/Si=2 aerogels.

Table 1

Summary of M and Si elemental analysis data for selected composite aerogels

M-oxide precursor	**calc. M/Si (mol/mol)**	**epoxide**	**wt% M**	**wt% Si**	**actual M/Si (mol/mol)**
Cr^{3+}	4	PO	28.5	3.7	4.2
Zr^{4+}	1	TMO	35.6	9.3	1.2
Nb^{5+}	5	TMO	49.9	2.8	5.4
W^{6+}	2	DMO	60.6	3.3	2.8

Table 2

Summary of synthetic conditions for the preparation of various M-Si mixed oxide nanocomposite gels

M^{x+}	M/Si (mol/mol)	epoxide	t_{gel}
Al^{3+}	3	PO	5 min
Al^{3+}	3	TMO	12 hr
Cr^{3+}	5	PO	4 min
Cr^{3+}	2	PO	4 min
Cr^{3+}	1	PO	6 min
Zr^{4+}	1	PO	1 min
Zr^{4+}	1	TMO	2 min
Hf^{4+}	1	TMO	15 min
Nb^{5+}	1	TMO	15 min
Ta^{5+}	1	TMO	1 min
W^{6+}	2	DMO	10 min

Table 3

Summary of N_2 adsorption/desorption results for various M-Si mixed oxide aerogels

M^{x+}	M/Si (mol/mol)	epoxide	surf. area (BET; m^2/g)	pore vol. (mL/g)	avg. pore diam. (nm)
Al^{3+}	3	PO	773	3.26	14.1
Al^{3+}	3	TMO	476	1.07	7.5
Cr^{3+}	5	PO	481	1.94	13.7
Cr^{3+}	2	PO	442	0.95	7.1
Cr^{3+}	1	PO	543	1.52	10.6
Zr^{4+}	1	PO	448	0.81	5.8
Zr^{4+}	1	TMO	477	0.83	5.7
Hf^{4+}	1	TMO	210	0.27	4.4
Nb^{5+}	1	TMO	403	0.98	9.1
Ta^{5+}	1	TMO	316	0.75	8.6
W^{6+}	2	DMO	90	0.39	16.3

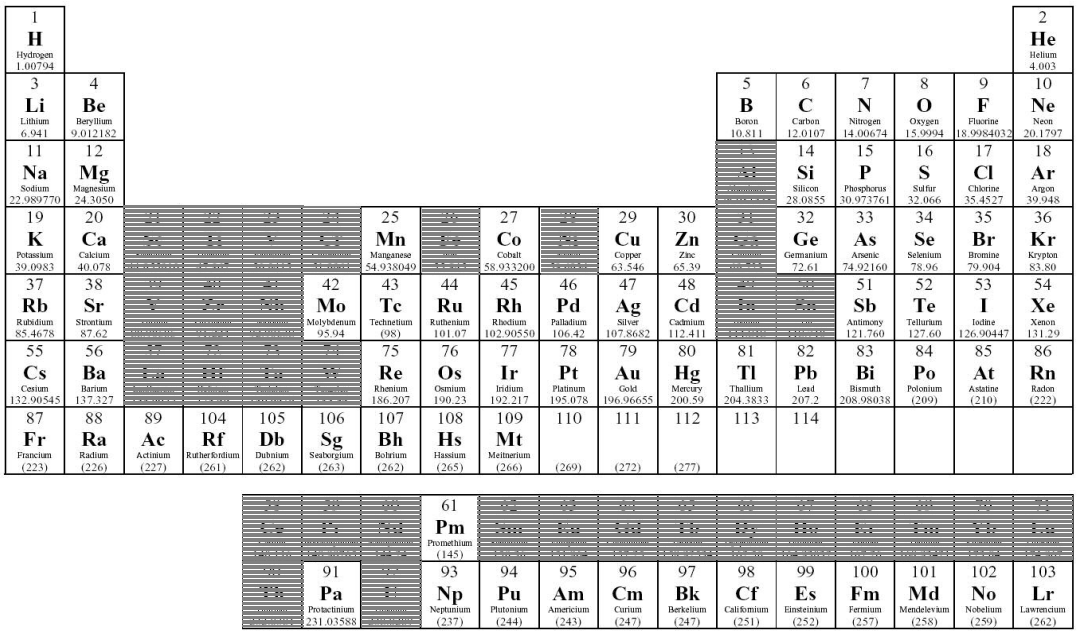

Figure 1. Summary of the metal oxides and M-Si mixed oxide composites prepared to date by the epoxide addition method (shaded).

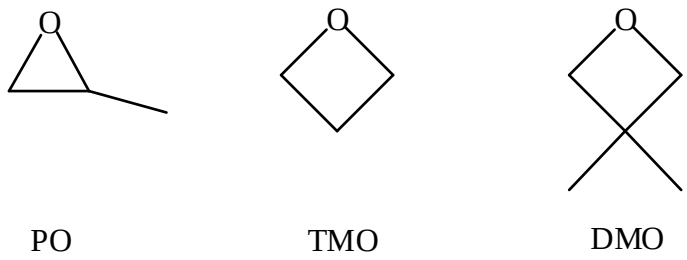

Figure 2. Structures of a 1,2-epoxide (PO) and 1,3-epoxides (TMO and DMO).

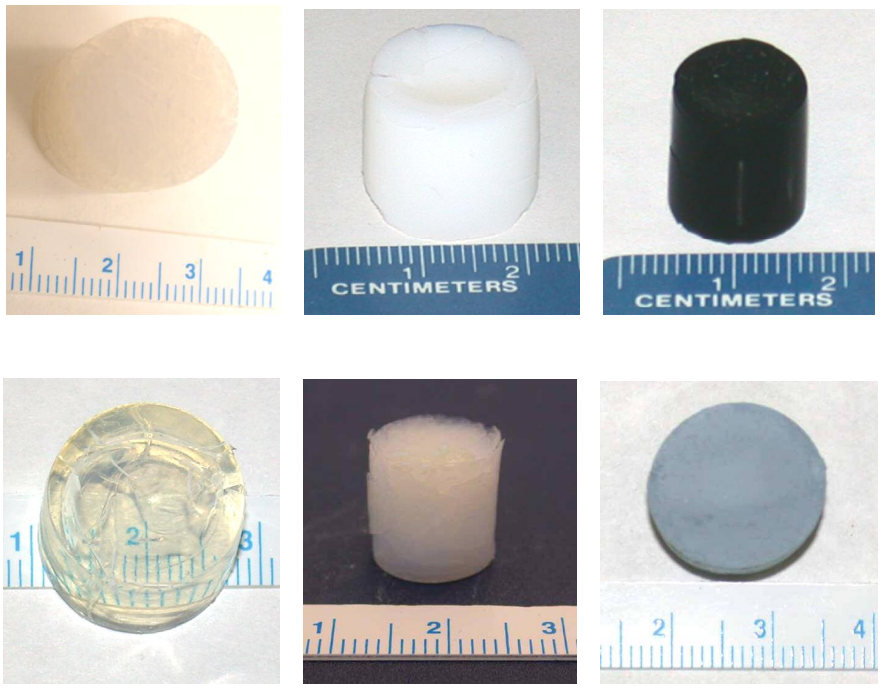

Figure 3. Pictures of various M-Si mixed oxide aerogel monoliths: left to right, top row, Al/Si=3, Sn/Si=2, Cr/Si=2; bottom row, Zr/Si=2, Nb/Si=5, W/Si=2. The scale in all pictures is in centimeters.

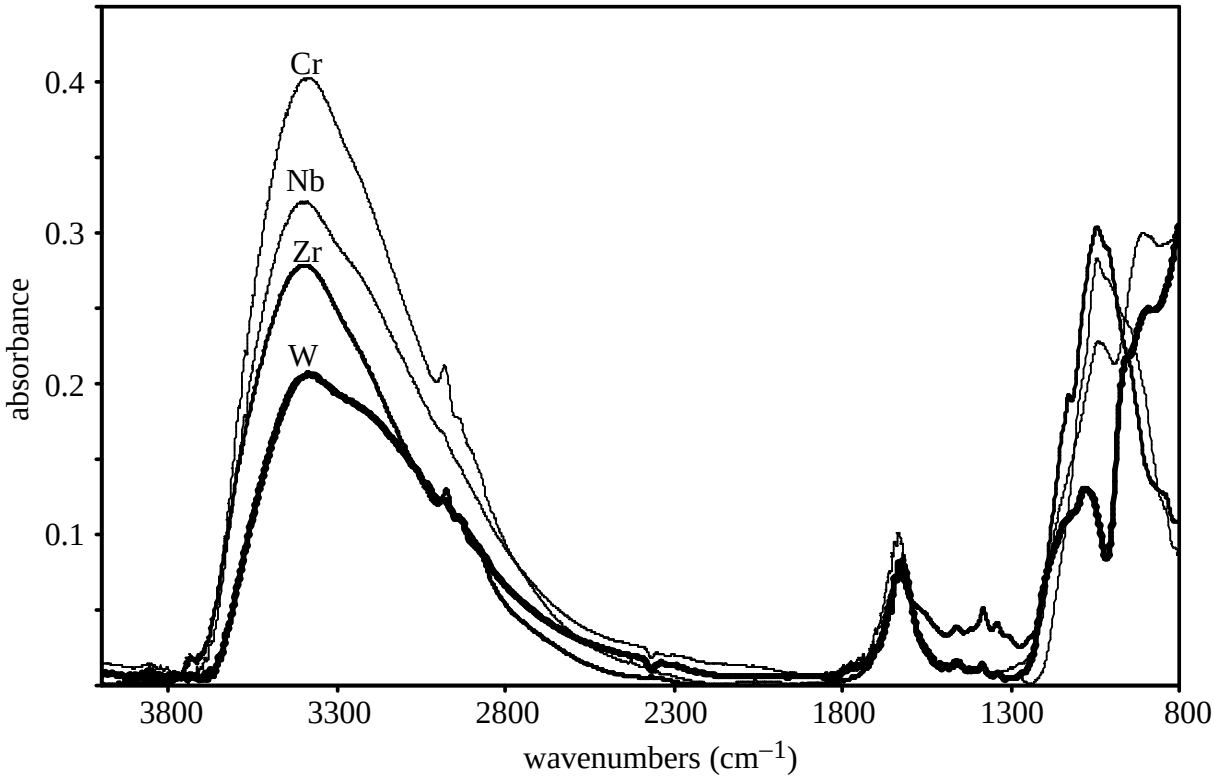

Figure 4. FTIR spectra of various M/Si=2 composites. The labels indicate the metal oxide present in each spectrum. The ν_{as}(Si–O–Si) peak for the compounds can be seen *c.a.* 1050 cm^{-1}. Peaks at energies >1000 cm^{-1} for the Nb and W composites are due to the metal oxide phase as confirmed by FTIR analysis of samples containing no SiO_2 component.

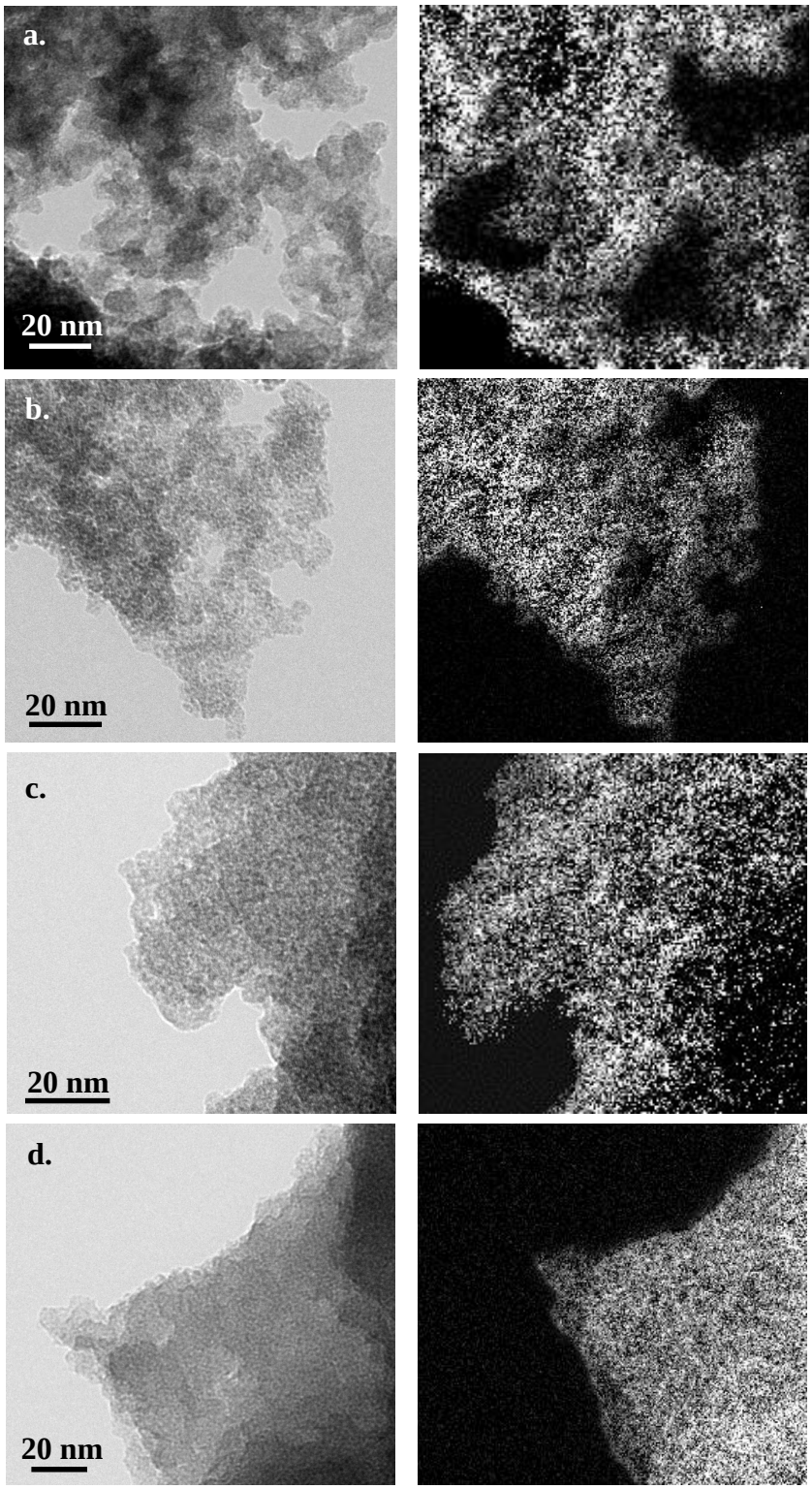

Figure 5. Bright field TEM images (left) and EFTEM Si maps (right) of a. W/Si = 2, b. Nb/Si=1, c. Zr/Si=1, and d. Cr/Si=2 aerogels.